7-2021

Muscle Force Contributions to Ankle Joint Contact Forces during an Unanticipated Cutting Task in People with Chronic Ankle Instability

Hoon Kim
Marquette University

Rianna M. Palmieri-Smith
University of Michigan - Ann Arbor

Kristof Kipp
Marquette University, kristof.kipp@marquette.edu

Journal of Biomechanics, Vol. 124 (July 19, 2021): 110566. DOI.

Muscle Force Contributions to Ankle Joint Contact Forces during an Unanticipated Cutting Task in People with Chronic Ankle Instability

Hoon Kim
Joint Department of Biomedical Engineering, University of North Carolina at Chapel Hill and North Carolina State University, Chapel Hill, NC
Riann Palmieri-Smith
School of Kinesiology, University of Michigan, Ann Arbor, MI
Orthopaedic and Rehabilitation Biomechanics Laboratory, University of Michigan, Ann Arbor, MI
Kristof Kipp
Department of Physical Therapy – Program in Exercise Science, Marquette University, Milwaukee, WI

Abstract

The purpose of this study was to compare muscle force contributions to ankle joint compression and anteroposterior shear forces between people with chronic ankle instability (CAI) and healthy controls (CON) during an unanticipated cutting task. Eleven people with CAI and 11 CON performed an unanticipated cutting task as three-dimensional motion capture, ground reaction force (GRF), and muscle activation data were collected. A musculoskeletal modeling was used to calculate talocrural joint compression and anteroposterior shear forces and parse out the contributions to these forces from ankle-spanning muscles and from GRF. Independent t-tests were used for statistical analysis. People with CAI exhibited greater anterior shear force peaks during early ($p = 0.048$, d = 0.98) and late ($p = 0.017$, d = 1.21) stance compared to CON. The difference in early stance shear force appeared to arise from greater GRF contribution ($p = 0.026$, d = 1.12) in CAI group, whereas the difference in late stance shear force appeared to arise from greater contribution of lateral gastrocnemius ($p = 0.026$, d = 1.12), medial gastrocnemius ($p = 0.048$, d = 0.98), tibialis posterior ($p = 0.017$, d = 1.22), fibularis brevis ($p = 0.035$, d = 1.05), and fibularis longus ($p = 0.023$, d = 1.15). People with CAI exhibit greater anterior shear, but not compressive forces in talocrural joint during an unanticipated cutting task. The differences in anterior shear force were the result of passive and active contributions from GRF during early stance and lower leg muscles during late stance, respectively.

Keywords

Biomechanics, Injury, Modelling, Simulation, Osteoarthritis

1. Introduction

Up to 70% of people who suffer a sprain of the lateral ligaments of the ankle joint complex develop chronic ankle instability (CAI) (Gribble et al., 2016, Herzog et al., 2019). CAI is characterized by repeated episodes or perceptions of the ankle giving away and persistent symptoms, such as pain and muscle weakness. A recent review of function in people with CAI suggested three categories of impairments: pathomechanical, sensory-perceptual impairments, and motor-behavioral impairments (Hertel and Corbett, 2019). In combination, these impairments result in persistent instability of the ankle, which in turn decreases the level of physical activity and quality of life in people with this condition and places them at risk for future injury or joint degeneration (Houston et al., 2014).

Ankle osteoarthritis, or degeneration of articular structures in the tibiotalar joints, is apparent in approximately 70% of patients with CAI (Hintermann et al., 2002) and its cause or causes remain unknown. One of the purported risk factors for the development and progression of osteoarthritis after CAI is a change in the magnitude of the joint contact forces (Lane Smith et al., 2000, Martin and Buckwalter, 2006). Simulation studies show that joint contact forces and stress increase in the presence of ankle ligament rupture or ankle joint malalignment (Bae et al., 2015, Kim and Kipp, 2020), which may in turn alter strain placed on joint structures and possibly result in accelerated degeneration of articular cartilage and subchondral bone. While these data provide insights into how ankle joint contact forces/stress may change in those with joint malalignment and acute ankle injury, the findings resulted from simulated malalignments and ligament ruptures based on healthy subjects. Only one recent study investigated joint loads in people with CAI (Li et al., 2019). That study, however, investigated differences in knee joint contact forces between people with and without CAI and found that both groups exhibited comparable tibiofemoral contact forces during a drop landing on a tilted surface. Although this study provides evidence that CAI does not affect contact forces at proximal joints (Li et al., 2019), which is clinically relevant for musculoskeletal injuries secondary to CAI (e.g., ACL injury), the effects of CAI on contact forces in the ankle joint are still not known. Furthermore, given that joint contact forces are the result of ground reaction forces (GRF) (Wang et al., 2017) and muscle forces (Herzog et al., 2003, Sasaki and Neptune, 2010), investigating their respective contributions to the ankle joint contact forces in people with CAI may identify specific ankle-spanning muscles that could be targeted during CAI rehabilitation to restore normal loading environment and possibly prevent the onset and progression of ankle osteoarthritis. A recent study quantified differences of muscle forces in people with and without CAI (Kim et al., 2021). And while the authors reported differences in the magnitudes of muscle forces, the contribution of muscles (e.g., ankle-spanning muscles) to the joint contact force in people with CAI is still unknown. However, aberrant muscle contributions to ankle joint contact force may be relevant to the greater risk of ankle osteoarthritis in people with CAI and would therefore fill a clinically important research gap.

Within the jumping and landing literature, researchers often use unanticipated cutting tasks to investigate the effects of cognitive demands on neuromuscular control in relation to musculoskeletal injury risk (Brown et al., 2009, Kim et al., 2020, McLean and Samorezov, 2009) (Almonroeder et al., 2018). Unanticipated cutting tasks also elicit movement strategies that are characterized by greater overall task demand (Wilke et al., 2020) and muscle activation magnitudes (Meinerz et al., 2015). Given that muscle activations are directly associated with joint contact forces (Steele et al., 2012), it would therefore be of interest to quantify joint contact force and muscle contributions during unanticipated cutting tasks in people with CAI. Therefore, the purpose of this study was to investigate the contributions of muscle forces and GRF to ankle joint compression and anteroposterior shear forces in people with and without CAI during an unanticipated cutting task. We hypothesized that the ankle joint compression and anteroposterior shear forces would be greater in people with CAI, and that the contribution of specific muscles to these forces would differ.

2. Methods

2.1. Participants

Twenty-two participants (11 people with CAI: 22.1 ± 3.2 years old, 1.68 ± 0.11 m, 69.0 ± 19.1 kg, 11 healthy controls (CON): 22.6 years old, 1.74 ± 0.11 m, 66.8 ± 15.5 kg) participated in this study. Each participant signed an informed consent form which was approved by University's Institutional Review Board. Inclusion criteria for the CAI group were based on a modified ankle instability instrument, with nine questions to quantify history of at least one significant ankle sprain and a history of either recurrent ankle sprains or symptoms (e.g., giving away episodes) (Hale and Hertel, 2005, Kipp and Palmieri-Smith, 2013, McVey et al., 2005). In addition, the Foot & Ankle Disability Index (FADI) (CAI: 90.3 ± 9.4; CON: 100 ± 0.0) and Foot & Ankle Disability Index in Sports (FADIS) (CAI: 88.6 ± 9.1; CON: 100 ± 0.0) were used to assess functional ability. A group of healthy controls were matched to the CAI group by sex, age, height, weight, and physical activity level which was based on Tegner scores. People with reported bilateral ankle sprains, fractures to the lower extremity, or significant current ankle of knee injuries that would have affected their performance were excluded (McVey et al., 2005).

2.2. Data collection procedures

All participants were outfitted with 32 reflective skin markers attached to their pelvis (anterior superior iliac spine, posterior superior iliac spine, iliac crest), femur (greater trochanter, medial and lateral epicondyle, anterior thigh), tibia (fibular head, lateral shank, medial and lateral malleoli), and foot (calcaneal tuberosity, 1st metatarsal base and head, 5th metatarsal head) (Brown et al., 2009, Kipp and Palmieri-Smith, 2012) and 5 electromyography (EMG) electrodes (Delsys, MA, USA) attached over the muscle bellies of the soleus, medial gastrocnemius, lateral gastrocnemius, tibialis anterior, and fibularis longus muscles.

Each participant was asked to perform three to five successful trials of unanticipated cutting. For this task, participants stood one leg length (distance between anterior superior iliac supine and medial malleolus) away from a landing area. Each participant performed a forward jump over a 15 cm box, landed on a single leg, and immediately executed a 90° cut away from the landing leg (Brown et al., 2009, McLean and Samorezov, 2009).

The landing leg and cutting direction were indicated by a visual stimulus that was displayed on a computer screen that was set at waist level just behind the force plate. The stimulus was triggered by the breaking of a light beam, which was positioned at the mid-point between the takeoff and position and the landing area (Kim et al., 2020). Therefore, the cutting direction and landing leg were unknown until participants broke the light beam. Each participant performed sufficient practice trials to be familiar with the tasks. Participants were asked to perform 3–5 successful trials of unanticipated cutting. A trial was counted as a successful trial when participants landed with their foot entirely on the force plate and cut in the correct direction at 90°.

Three-dimensional positions of the reflective markers were collected with motion capture cameras (ViconMx, CA, USA) at a sampling frequency of 240 Hz. Muscle activations were recorded with EMG at a sampling frequency of 1200 Hz. GRF were recorded with an in-ground force plate (Advanced Medical Technologies Inc., MA, USA) at a sampling frequency of 1200 Hz.

2.3. Data processing procedures

The position of skin markers and GRF data were both lowpass-filtered with Butterworth filter at a cutoff frequency of 12 Hz. Muscle activation data were bandpass-filtered with Butterworth filters at cutoff frequencies of 20 and 450 Hz. The filtered muscle activation data were further smoothed with an additional lowpass Butterworth filter at a cutoff frequency of 10 Hz. We defined the beginning and end of stance phase based on the time points when the vertical GRF rose above and fell below 10 N, respectively. The amplitudes of the smoothed muscle activation data were normalized by the maximum activation of each signal and time-normalized (0 to 100%) to the duration of the stance phase of the cutting task.

The analysis consisted of a standard OpenSim processing pipeline (Fig. 1) (Delp et al., 2007). A musculoskeletal model with 23°-of-freedom and 92 muscle actuators was scaled to the static trial of each subject (Delp et al., 1990). The scaling process created a subject-specific model for each participant based on their respective anthropometrics (e.g., segment lengths) (Fig. 1A). The maximum isometric muscle forces within the generic model were initially scaled via generic (C) and subject-specific (S) multipliers that were based on each participant's estimated muscle volume, which in turn were based on their respective body mass and height (Eqs. (1), (2), and (3)) (Handsfield et al., 2014).

(1)

$$F_{Subject}^{MaxIso} = F_{Generic}^{MaxIso} \times (C \times S)$$

(2)

$$S = \frac{MuscleVolume_{Subject}}{MuscleVolume_{Model}}$$

(3)

$$MuscleVolume = (47 \times BodyMass \times BodyHeight) + 1285$$

The inverse kinematics (IK) tool was used to calculate the joint angles by minimizing differences between virtual model markers and experimental subject markers (Fig. 1. B). Static optimization (SO) was used to estimate muscle forces and activations by minimizing the sum of squared activations of each muscle (Fig. 1C). The three-dimensional ankle joint contact forces were computed with the joint reaction analysis tool (Fig. 1E), which used the subject-specific model, IK kinematics, SO-based muscle forces, and GRF data (Steele et al., 2012). The joint reaction analysis tool was used to calculate the contribution of individual ankle muscles (soleus, lateral gastrocnemius, medial gastrocnemius, tibialis posterior, tibialis anterior, fibularis brevis, and fibularis longus) and GRF to the three-dimensional ankle joint contact forces in talocrural joint (Fig. 1F) (Maniar et al., 2018).

Given the absence of maximum voluntary isometric contractions, the simulated muscle activations were validated against the processed experimental EMG data through visual inspection and comparison of the muscle activation patterns (Fig. 1D and Fig. 2) (Hamner et al., 2010, Hicks et al., 2015).

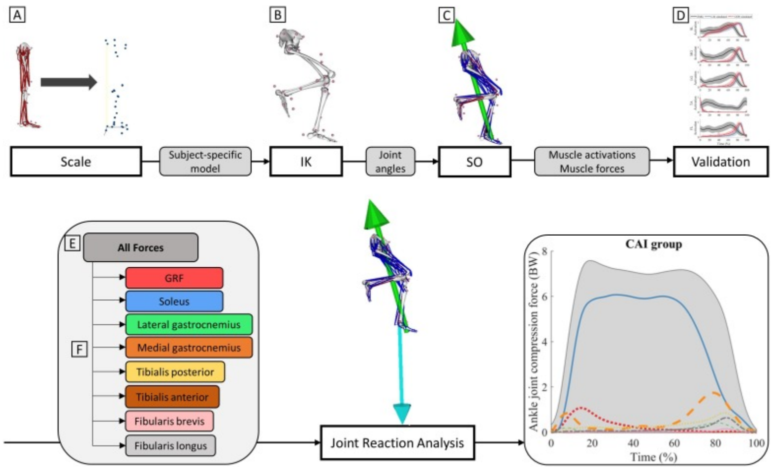

Fig. 1. Workflow. A: scaling of model. B: inverse kinematics (IK). C: static optimization (SO). D: validation by comparing pattern of measured muscle activation and simulated activation. E: joint reaction analysis with all forces (e.g., ground reaction force (GRF) and individual muscle). F: separate joint reaction analysis for each force (e.g., GRF or individual muscle).

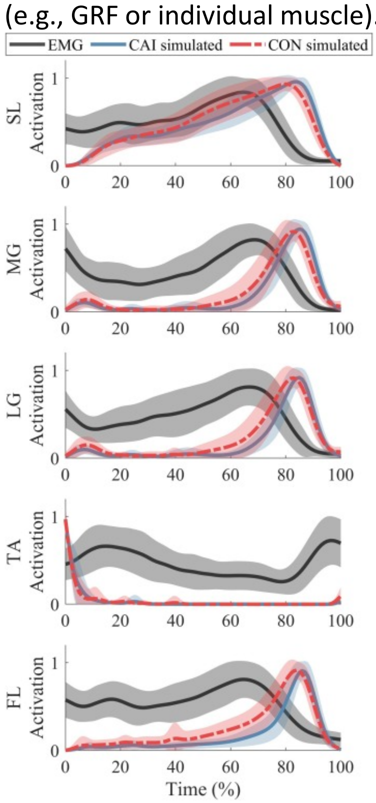

Fig. 2. Mean ± SD normalized muscle activations from EMG and simulation in people with chronic ankle instability (CAI) and healthy controls (CON) during unanticipated cutting. SL: soleus, MG: medial gastrocnemius, LG: lateral gastrocnemius, TA: tibialis anterior, FL: fibularis longus.

The ankle joint contact forces and the respective contributions from the individual muscles and the GRF were normalized by the bodyweight of each subject. The ankle joint compression forces exhibited only one peak during the stance phase of the cutting task, while the anteroposterior shear forces exhibited three distinct peaks (i.e., peaks in anterior shear force during early (~first 20% of stance) and late stance (~last 80% of stance), and a peak in posterior shear force during mid stance) (Fig. 3). The shear forces in the mediolateral direction were negligible and were therefore excluded from further analysis. The discrete peak ankle joint contact forces were extracted and averaged across three trials. In addition, the contributions from each muscle and the GRF at the time of the peak ankle joint contact forces were also extracted and likewise averaged across the same three trials.

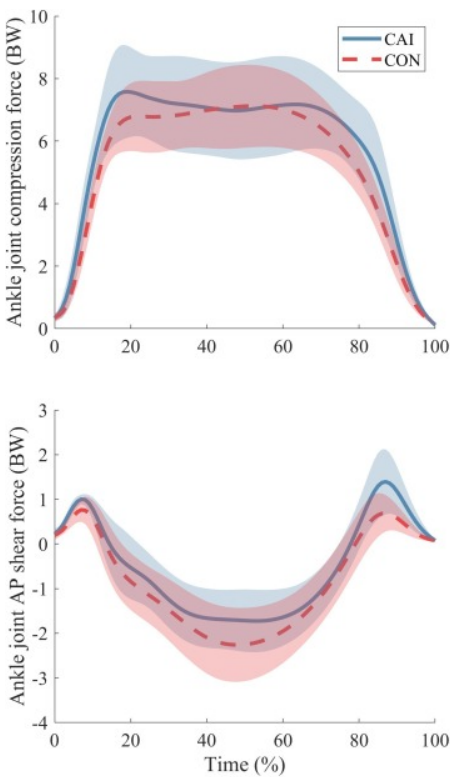

Fig. 3. Mean ± SD normalized time-series ankle joint compression force (top) and anteroposterior shear force (bottom) in people with chronic ankle instability (CAI) and healthy controls (CON) during unanticipated cutting.

2.4. Statistical analysis

The independent variable for the statistical analysis was group (CAI vs CON). The dependent variables for the statistical analysis were peak ankle joint compression force, the three stance phase specific anteroposterior shear forces, and the respective force contributions from all individual muscles and GRF to the peak ankle joint contact forces at the previously identified instances. The normality of all dependent variables was assessed with the Kolmogorov–Smirnov test (Öner and Deveci Kocakoç, 2017). Independent t-tests were used to compare dependent variables between the CAI and CON groups. The alpha level was set at 0.05. Effect sizes (Cohen's *d*) were also calculated for each comparison. Cohen's *d* was considered small if between 0.2 and 0.5, medium if between 0.5 and 0.8, and large if greater than 0.8 (Cohen, 2013). All statistical analyses were performed in MATLAB (MathWorks, MA, USA).

3. Results

The ankle joint compression and anteroposterior shear forces and the contributions of GRF and muscles to the ankle joint contact forces during the unanticipated cutting task are shown in Fig. 3 and Fig. 4, respectively.

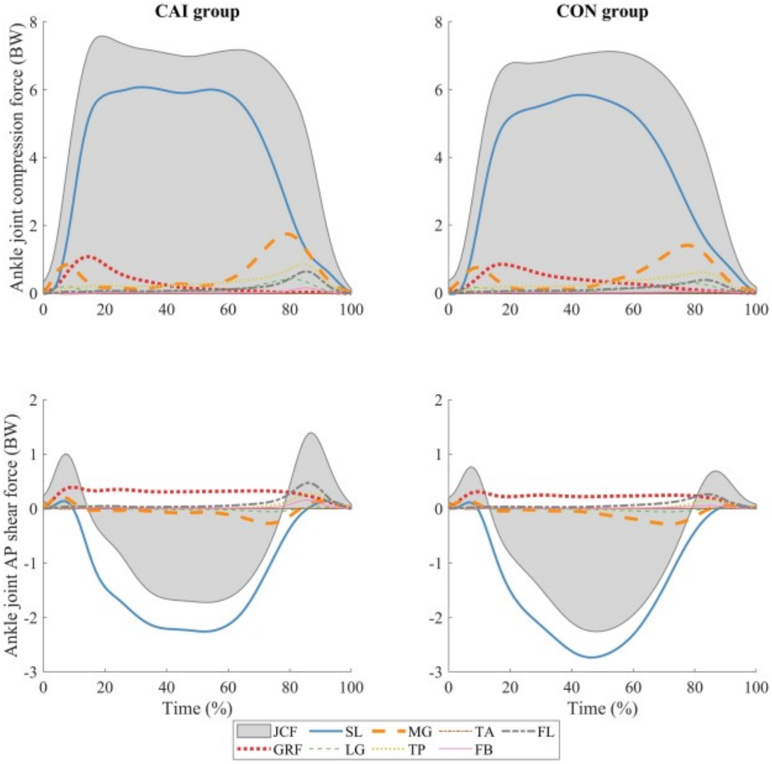

Fig. 4. Averaged and normalized ankle joint compression (top row) and anteroposterior (bottom row) forces and contributions from ground reaction forces and individual muscles in people with chronic ankle instability (CAI) and healthy controls (CON) during anticipated cutting. JCF: joint contact force, GRF: ground reaction force, SL: soleus, MG: medial gastrocnemius, LG: lateral gastrocnemius, TP: tibialis posterior, TA: tibialis anterior, FB: fibularis brevis, FL: fibularis longus.

3.1. Ankle joint compression forces

No significant difference was identified between the CAI and CON groups for the peak compression force during unanticipated cutting (p = 0.307, Cohen's d = 0.484) (Fig. 5). Furthermore, there were no significant differences between the CAI and CON groups in the force contributions from the individual muscles or GRF to peak ankle joint compression force (p = 0.247–866, Cohen's d = 0.079–0.550) (Fig. 6).

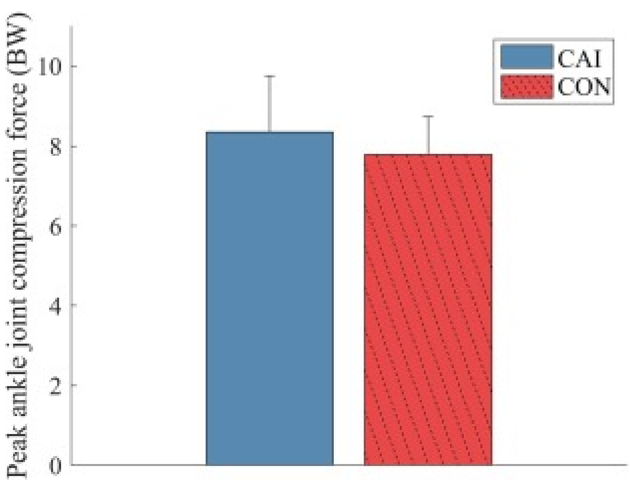

Fig. 5. Mean ± SD peak ankle joint compression forces in people with chronic ankle instability (CAI) and healthy controls (CON) during unanticipated cutting.

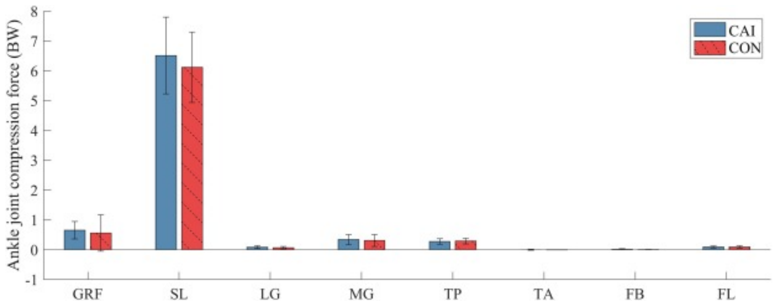

Fig. 6. Mean ± SD normalized contribution of ground reaction force and individual muscles at time of peak ankle joint compression force in people with chronic ankle instability (CAI) and healthy controls (CON) during unanticipated cutting. JCF: joint contact force, GRF: ground reaction force, SL: soleus, MG: medial gastrocnemius, LG: lateral gastrocnemius, TP: tibialis posterior, TA: tibialis anterior, FB: fibularis brevis, FL: fibularis longus.

3.2. Ankle joint anteroposterior shear forces

Significant differences were noted between the CAI and CON groups for the first (*p* = 0.048, Cohen's d = 0.98) and third (*p* = 0.017, Cohen's d = 1.21) peaks in anteroposterior shear forces during unanticipated cutting (Fig. 7). Specifically, the two peaks in anterior shear forces in the CAI group were approximately 30% and 92% greater in the CON group. In contrast, there was no significant difference of the second peaks in anteroposterior shear forces between groups (*p* = 0.190, Cohen's d = 0.627) (Fig. 7).

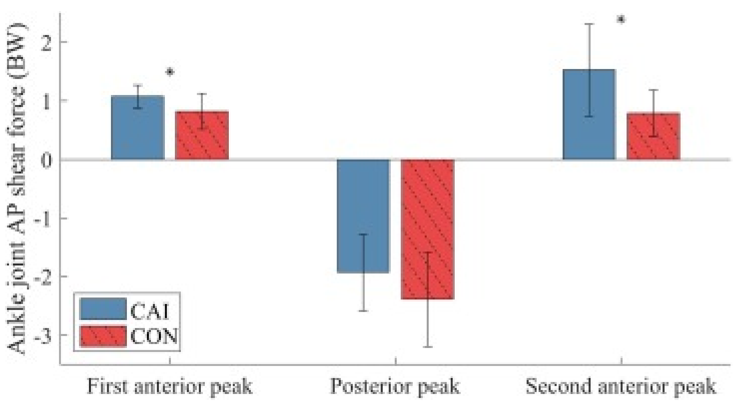

Fig. 7. Mean ± SD peak ankle joint anteroposterior forces in people with chronic ankle instability (CAI) and healthy controls (CON) during unanticipated cutting. *: significant difference with $p < 0.05$.

The contribution of individual muscles and GRF to the first and second peaks in anterior shear forces were also significantly different between the CAI and CON groups (Fig. 8). Specifically, people with CAI exhibited greater contribution from the GRF to the first peak in anterior shear force (*p* = 0.026, Cohen's d = 1.12) (Fig. 8). Furthermore, people with CAI exhibited greater contributions from the lateral gastrocnemius (*p* = 0.026, Cohen's d = 1.12), medial gastrocnemius (*p* = 0.048, Cohen's d = 0.98), tibialis posterior (*p* = 0.017, Cohen's d = 1.22), fibularis brevis (*p* = 0.035, Cohen's d = 1.05), and fibularis longus (*p* = 0.023, Cohen's d = 1.15) to the second peak in anterior shear force (Fig. 8).

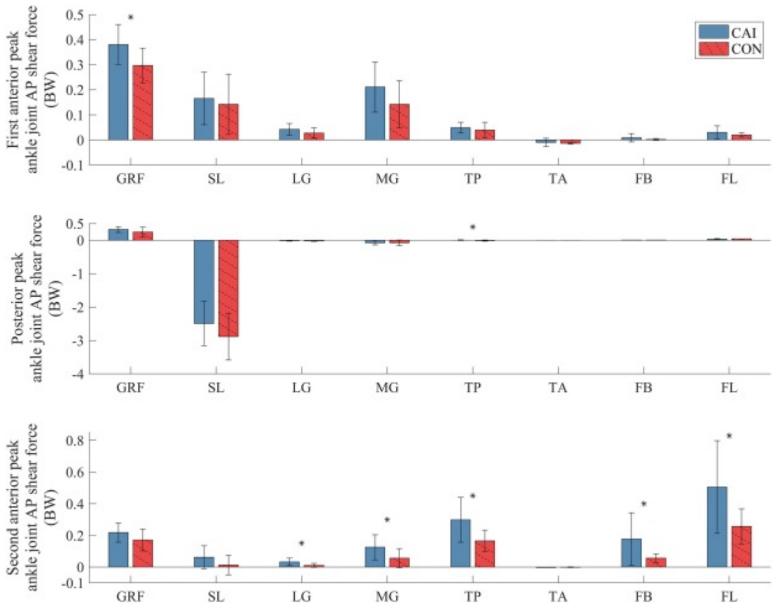

Fig. 8. Mean ± SD normalized contribution of ground reaction force and individual muscles at time of first anterior, posterior, and second anterior peaks of ankle joint anteroposterior (AP) shear force in people with chronic ankle instability (CAI) and healthy controls (CON) during unanticipated cutting. JCF: joint contact force, GRF: ground reaction force, SL: soleus, MG: medial gastrocnemius, LG: lateral gastrocnemius, TP: tibialis posterior, TA: tibialis anterior, FB: fibularis brevis, FL: fibularis longus, *: significant difference with $p < 0.05$.

4. Discussion

To our knowledge, this study is the first study to quantify the ankle joint contact force and muscle contribution to the ankle joint contact force during a dynamic task in people with CAI. Specifically, the current study investigated the ankle joint compression and anteroposterior shear forces in persons with and without CAI during an unanticipated cutting task and examined the contributions from the muscle forces and GRF to ankle joint compression and anteroposterior shear forces. We found that people with CAI exhibited greater peaks of ankle joint anterior shear, but not compression forces when compared to the CON group. In addition, people with CAI exhibited greater contribution from GRF to the first peak in ankle joint anterior shear force during early stance, and exhibited greater contribution from lower leg muscles to the second peak in ankle joint anterior shear force during late stance. Together, these results partially supported our hypotheses in that some ankle joint contact forces were greater in people with CAI, and in that these differences were the result of different stance phase specific contributions from individual muscles and GRF.

A primary finding of the current study was that people with CAI exhibited greater ankle joint anterior shear forces during unanticipated cutting compared to people in a CON group. The observed differences in anterior shear forces were also associated with a large effect size, which suggests that the differences are both significant and clinically meaningful. This finding is important because previous studies indicated that ankle joint shear forces are strongly associated with the progression of ankle osteoarthritis (Cohen et al., 1998, Lane Smith et al., 2000). Interestingly, findings from the current study suggest that the differences in anterior shear forces are the result of stance-phase specific muscle and GRF contributions. Specifically, people with CAI exhibited greater GRF contribution to the first peak in anterior ankle joint shear force compared to people in CON group. The first peak in anterior shear force occurred immediately after foot touchdown during the early stance phase of the cutting task. This phase is also associated with an impact transient in the GRF, which may contribute to the first peak in anterior shear force as the tibia pushes forward against a relatively fixed talus during the landing phase of the cutting task. Previous studies suggest that people with CAI land with protective movement strategies that are characterized by stiffening the ankle joint (i.e., restriction of ankle motion by co-contracting ankle-spanning muscles) and adopting a more close-packed ankle position (i.e., maximizing congruency of the ankle joint due to dorsiflexion) (Son et al., 2017), which could arguably lead to greater peaks in anterior shear force during the early stance phase of cutting. Consequently, this result may indicate that the arthrokinematics and protective movement strategies in people with CAI are partially responsible for the greater peak anterior ankle joint shear forces during the early stance phase of unanticipated cutting.

Another important finding relates to the group differences in phase-specific contributions by individual muscles to the anterior ankle joint shear forces in people with CAI. Specifically, several muscles exhibited between-group differences with large effect sizes at the time of the second peak in anterior ankle joint shear force. This result supports our initial hypothesis and suggests that the greater observed peak in anterior shear force at the ankle joint in people with CAI is the results of different muscle contributions. Greater anterior shear force contributions were observed in some of the plantar flexor (lateral gastrocnemius, medial gastrocnemius, and tibialis posterior) and evertor (fibularis brevis and fibularis longus) muscles during the late stance phase of unanticipated cutting in people with CAI. Notably, the fibularis longus and brevis as well as the tibialis posterior appeared to be the largest contributors to the anterior shear force at the ankle and exhibited the greatest differences in force contributions between the CAI and CON groups. Given that the fibularis longus and brevis are often implicated within the etiology and impairments associated with CAI these findings are perhaps not surprising (Donnelly et al., 2017, McLeod et al., 2015), but uniquely underscore the importance of restoring appropriate ankle joint function from a mechanical and clinical perspective because these results provide direct links between aberrant ankle joint shear forces and muscle actions. Researchers and clinicians should thus try to establish if restoring fibularis longus function normalizes anterior shear forces and helps mitigate the progression of ankle osteoarthritis in people with CAI.

There are some limitations associated with the methods and results of this study. First, the musculoskeletal model used in the current study does not account for the gliding-sliding joint kinematics of the talocrural joint, including more degrees-of-freedom into the musculoskeletal model may produce more realistic ankle joint kinematics and reveal additional details about joint loads and contributions from muscles. Second, only lower leg muscles were included in the estimating of the muscular contributions to ankle joint contact forces. Given that muscles that do not span a joint can still contribute to the contact force at that joint (Maniar et al., 2018), including and estimating the effects from other (more proximal) muscles (e.g., quadriceps or gluteus maximus) may provide more additional information for clinicians about which muscles may serve as targets during rehabilitation protocols. Third, the ankle joint shear forces in the mediolateral direction were not considered in the current study. Although mediolateral shear forces in the joint may also damage the joint articular tissue (Cohen et al., 1998), the magnitudes of the mediolateral shear forces in the current study were much smaller (e.g., peak mediolateral shear force was approximately 25% of peak anteroposterior shear force.) than the joint contact forces in the other two directions, which led us to exclude them in the current context. Lastly, the results of the current study are based on a sample of 22 people, which could be considered a relatively small sample. Given the general need for replication and extension of research into the areas mentioned above, future studies may thus also consider recruiting larger samples of people with CAI. Additional considerations and directions for future research also relate to the development and use of more detailed and subject-specific models based on a patient's ankle joint morphology with e.g., X-ray or fluoroscopy. Further, the unanticipated cutting task that was chosen for this investigation is an example of a common high-intensity sport task. However, investigating joint contact forces and the specific muscle and GRF contributions during activities of daily living (e.g., walking) may also provide additional insights about how to ameliorate deleterious joint loading and mitigate the progression of ankle osteoarthritis in people with CAI in the long-term (Lenton et al., 2018).

5. Conclusion

This study compared joint contact forces and the respective contribution of individual muscles and GRF between people with and without CAI. People with CAI exhibited greater anterior shear forces in the ankle during the early and late stance phases than people without CAI. Furthermore, the greater anterior shear forces were the result of greater GRF contribution during the early stance phase and greater muscle contribution during the late stance phase. It is suggested that clinicians and researchers investigate if targeting these stance phase specific contributions provides a way to also decrease anterior shear forces in an effort to eventually prevent ankle osteoarthritis in people with CAI.

Declaration of Competing Interest

The authors declare that they have no known competing financial interests or personal relationships that could have appeared to influence the work reported in this paper.

Acknowledgements

The authors would like to acknowledge assistance from the National Institutes of Health (T32 HD007422-20) and a research stipend from the NIDRR.

References

Almonroeder et al., 2018. T.G. Almonroeder, T. Kernozek, S. Cobb, B. Slavens, J. Wang, W. Huddleston. **Cognitive Demands Influence Lower Extremity Mechanics During a Drop Vertical Jump Task in Female Athletes.** J. Orthop. Sports Phys. Ther., 48 (2018), pp. 381-387

Bae et al., 2015. J.Y. Bae, K.S. Park, J.K. Seon, I. Jeon. **Analysis of the Effects of Normal Walking on Ankle Joint Contact Characteristics After Acute Inversion Ankle Sprain.** Ann. Biomed. Eng., 43 (2015), pp. 3015-3024

Brown et al., 2009. T.N. Brown, R.M. Palmieri-Smith, S.G. McLean. **Sex and limb differences in hip and knee kinematics and kinetics during anticipated and unanticipated jump landings: implications for anterior cruciate ligament injury.** Br. J. Sports Med., 43 (2009), pp. 1049-1056

Cohen, 2013. J. Cohen. **Statistical power analysis for the behavioral sciences.** Academic press (2013)

Cohen et al., 1998. N.P. Cohen, R.J. Foster, V.C. Mow. **Composition and dynamics of articular cartilage: structure, function, and maintaining healthy state.** J. Orthop. Sports Phys. Ther., 28 (1998), pp. 203-215

Delp et al., 2007. S.L. Delp, F.C. Anderson, A.S. Arnold, P. Loan, A. Habib, C.T. John, E. Guendelman, D.G. Thelen. **OpenSim: open-source software to create and analyze dynamic simulations of movement.** IEEE Trans. Biomed. Eng., 54 (2007), pp. 1940-1950

Delp et al., 1990. S.L. Delp, J.P. Loan, M.G. Hoy, F.E. Zajac, E.L. Topp, J.M. Rosen. **An interactive graphics-based model of the lower extremity to study orthopaedic surgical procedures.** IEEE Trans. Biomed. Eng., 37 (1990), pp. 757-767

Donnelly et al., 2017. L. Donnelly, L. Donovan, J.M. Hart, J. Hertel. **Eversion Strength and Surface Electromyography Measures With and Without Chronic Ankle Instability Measured in 2 Positions.** Foot Ankle Int., 38 (2017), pp. 769-778

Gribble et al., 2016. P.A. Gribble, C.M. Bleakley, B.M. Caulfield, C.L. Docherty, F. Fourchet, D.T. Fong, J. Hertel, C.E. Hiller, T.W. Kaminski, P.O. McKeon, K.M. Refshauge, E.A. Verhagen, B.T. Vicenzino, E.A. Wikstrom, E. Delahunt. **Evidence review for the 2016 International Ankle Consortium consensus statement on the prevalence, impact and long-term consequences of lateral ankle sprains.** Br J Sports Med, 50 (2016), pp. 1496-1505

Hale and Hertel, 2005. S.A. Hale, J. Hertel. **Reliability and Sensitivity of the Foot and Ankle Disability Index in Subjects With Chronic Ankle Instability.** J Athl Train, 40 (2005), pp. 35-40

Hamner et al., 2010. S.R. Hamner, A. Seth, S.L. Delp. **Muscle contributions to propulsion and support during running.** J. Biomech., 43 (2010), pp. 2709-2716

Handsfield et al., 2014. G.G. Handsfield, C.H. Meyer, J.M. Hart, M.F. Abel, S.S. Blemker. **Relationships of 35 lower limb muscles to height and body mass quantified using MRI.** J. Biomech., 47 (2014), pp. 631-638

Hertel and Corbett, 2019. J. Hertel, R.O. Corbett. **An Updated Model of Chronic Ankle Instability.** J Athl Train, 54 (2019), pp. 572-588

Herzog et al., 2019. M.M. Herzog, Z.Y. Kerr, S.W. Marshall, E.A. Wikstrom. **Epidemiology of Ankle Sprains and Chronic Ankle Instability.** J Athl Train, 54 (2019), pp. 603-610

Herzog et al., 2003. W. Herzog, D. Longino, A. Clark. **The role of muscles in joint adaptation and degeneration.** Langenbecks Arch. Surg., 388 (2003), pp. 305-315

Hicks et al., 2015. J.L. Hicks, T.K. Uchida, A. Seth, A. Rajagopal, S.L. Delp. **Is my model good enough? Best practices for verification and validation of musculoskeletal models and simulations of movement.** J. Biomech. Eng., 137 (2015), Article 020905

Hintermann et al., 2002. B. Hintermann, A. Boss, D. Schafer. **Arthroscopic findings in patients with chronic ankle instability.** Am. J. Sports Med., 30 (2002), pp. 402-409

Houston et al., 2014. M.N. Houston, B.L. Van Lunen, M.C. Hoch. **Health-related quality of life in individuals with chronic ankle instability.** J. Athl. Train., 49 (2014), pp. 758-763

Kim and Kipp, 2020. H. Kim, K. Kipp. **Simulated anterior translation and medial rotation of the talus affect ankle joint contact forces during vertical hopping.** Comput. Methods Biomech. Biomed. Engin, 23 (2020), pp. 484-490

Kim et al., 2020. H. Kim, R. Palmieri-Smith, K. Kipp. **Time-frequency analysis of muscle activation patterns in people with chronic ankle instability during Landing and cutting tasks.** Gait Posture, 82 (2020), pp. 203-208

Kim et al., 2021. H. Kim, R. Palmieri-Smith, K. Kipp. **Peak Forces and Force Generating Capacities of Lower Extremity Muscles During Dynamic Tasks in People With and Without Chronic Ankle Instability.** Sports Biomech. (2021), pp. 1-14

Kipp and Palmieri-Smith, 2012. K. Kipp, R.M. Palmieri-Smith. **Principal component based analysis of biomechanical inter-trial variability in individuals with chronic ankle instability.** Clin. Biomech. (Bristol, Avon), 27 (2012), pp. 706-710

Kipp and Palmieri-Smith, 2013. K. Kipp, R.M. Palmieri-Smith. **Differences in kinematic control of ankle joint motions in people with chronic ankle instability.** Clin. Biomech. (Bristol, Avon), 28 (2013), pp. 562-567

Lane Smith et al., 2000. R. Lane Smith, M.C. Trindade, T. Ikenoue, M. Mohtai, P. Das, D.R. Carter, S.B. Goodman, D.J. Schurman. **Effects of shear stress on articular chondrocyte metabolism.** Biorheology, 37 (2000), pp. 95-107

Lenton et al., 2018. G.K. Lenton, P.J. Bishop, D.J. Saxby, T.L.A. Doyle, C. Pizzolato, D. Billing, D.G. Lloyd. **Tibiofemoral joint contact forces increase with load magnitude and walking speed but remain almost unchanged with different types of carried load.** PLoS One, 13 (2018), Article e0206859

Li et al., 2019. Y. Li, H. Wang, K.J. Simpson. **Chronic Ankle Instability Does Not Influence Tibiofemoral Contact Forces During Drop Landings Using a Musculoskeletal Model.** J. Appl. Biomech. (2019), pp. 1-5

Maniar et al., 2018. N. Maniar, A.G. Schache, P. Sritharan, D.A. Opar. **Non-knee-spanning muscles contribute to tibiofemoral shear as well as valgus and rotational joint reaction moments during unanticipated sidestep cutting.** Sci. Rep., 8 (2018), p. 2501

Martin and Buckwalter, 2006. J.A. Martin, J.A. Buckwalter. **Post-traumatic osteoarthritis: the role of stress induced chondrocyte damage.** Biorheology, 43 (2006), pp. 517-521

McLean and Samorezov, 2009. S.G. McLean, J.E. Samorezov. **Fatigue-induced ACL injury risk stems from a degradation in central control.** Med. Sci. Sports Exerc., 41 (2009), pp. 1661-1672

McLeod et al., 2015. M.M. McLeod, P.A. Gribble, B.G. Pietrosimone. **Chronic Ankle Instability and Neural Excitability of the Lower Extremity.** J Athl Train, 50 (2015), pp. 847-853

McVey et al., 2005. E.D. McVey, R.M. Palmieri, C.L. Docherty, S.M. Zinder, C.D. Ingersoll. **Arthrogenic muscle inhibition in the leg muscles of subjects exhibiting functional ankle instability.** Foot Ankle Int., 26 (2005), pp. 1055-1061

Meinerz et al., 2015. C.M. Meinerz, P. Malloy, C.F. Geiser, K. Kipp. **Anticipatory Effects on Lower Extremity Neuromechanics During a Cutting Task.** J Athl Train, 50 (2015), pp. 905-913

Öner and Deveci Kocakoç, 2017. M. Öner, İ. Deveci Kocakoç. **Jmasm 49: A compilation of some popular goodness of fit tests for normal distribution: Their algorithms and matlab codes (matlab).** J. Modern Appl. Statistical Methods, 16 (2017), p. 30

Sasaki and Neptune, 2010. K. Sasaki, R.R. Neptune. **Individual muscle contributions to the axial knee joint contact force during normal walking.** J. Biomech., 43 (2010), pp. 2780-2784

Son et al., 2017. S.J. Son, H. Kim, M.K. Seeley, J.T. Hopkins. **Movement Strategies among Groups of Chronic Ankle Instability, Coper, and Control.** Med. Sci. Sports Exerc., 49 (2017), pp. 1649-1661

Steele et al., 2012. K.M. Steele, M.S. Demers, M.H. Schwartz, S.L. Delp. **Compressive tibiofemoral force during crouch gait.** Gait Posture, 35 (2012), pp. 556-560

Wang et al., 2017. X. Wang, Y. Ma, B.Y. Hou, W.K. Lam. **Influence of Gait Speeds on Contact Forces of Lower Limbs.** J Healthc Eng, 2017 (2017), p. 6375976

Wilke et al., 2020. J. Wilke, D. Groneberg, W. Banzer, F. Giesche. **Perceptual-Cognitive Function and Unplanned Athletic Movement Task Performance: A Systematic Review.** Int. J. Environ. Res. Public Health, 17 (2020)